The AAPS Journal (2024) 26:33
https://doi.org/10.1208/s12248-024-00899-6

RESEARCH ARTICLE

Biodistribution of Drug/ADA Complexes: The Impact of Immune Complex Formation on Antibody Distribution

Eugenia Opolka-Hoffmann[1] · Martin R. Edelmann[2,3] · Michael B. Otteneder[4] · Simon Hauri[4] · Gregor Jordan[1] · Peter Schrag[4] · Martin Lechmann[1] · Gerhard Winter[5] · Roland F. Staack[1]

Received: 8 December 2023 / Accepted: 10 February 2024 / Published online: 13 March 2024

Abstract

The clinical use of therapeutic monoclonal antibodies (mAbs) for the treatment of cancer, inflammation, and other indications has been successfully established. A critical aspect of drug-antibody pharmacokinetics is immunogenicity, which triggers an immune response via an anti-drug antibody (ADA) and forms drug/ADA immune complexes (ICs). As a consequence, there may be a reduced efficacy upon neutralization by ADA or an accelerated drug clearance. It is therefore important to understand immunogenicity in biological therapies. A drug-like immunoglobulin G (IgG) was radiolabeled with tritium, and ICs were formed using polyclonal ADA, directed against the complementary-determining region of the drug-IgG, to investigate *in vivo* biodistribution in rodents. It was demonstrated that 65% of the radioactive IC dose was excreted within the first 24 h, compared with only 6% in the control group who received non-complexed ^{3}H-drug. Autoradiographic imaging at the early time point indicated a deposition of immune complexes in the liver, lung, and spleen indicated by an increased radioactivity signal. A biodistribution study confirmed the results and revealed further insights regarding excretion and plasma profiles. It is assumed that the immune complexes are readily taken up by the reticuloendothelial system. The ICs are degraded proteolytically, and the released radioactively labeled amino acids are redistributed throughout the body. These are mainly renally excreted as indicated by urine measurements or incorporated into protein synthesis. These biodistribution studies using tritium-labeled immune complexes described in this article underline the importance of understanding the immunogenicity induced by therapeutic proteins and the resulting influence on biological behavior.

Keywords biodistribution · immune complexes · pharmacokinetics · radiolabeling · tritium

Introduction

Monoclonal antibodies (mAbs) and other biotherapeutics enable the targeted treatment of a broad spectrum of diseases (1). While great efforts are being made in drug development to reduce the immunogenicity of antibody therapeutics, this liability remains challenging. Undesirable events such as abrogation of pharmacologic effects or hypersensitivity reactions can be triggered by the binding of anti-drug antibodies (ADAs) to the circulating drug (2). ADAs can act in a neutralizing or non-neutralizing manner. Neutralization of therapeutic mAbs is largely driven by the binding of ADAs to the complementary-determining region (CDR) and can consequently lead to the abrogation of pharmaceutical activity (3, 4). These ADAs, which target the CDR of a therapeutic mAb, have been reported from both humanized and fully human molecules (5, 6). In addition to hindering the binding of the drug to its target, the formation of ADA can lead to

✉ Eugenia Opolka-Hoffmann
Eugenia.opolka-hoffmann@roche.com

1 Roche Pharma Research and Early Development, Pharmaceutical Sciences, Roche Innovation Center Munich, Roche Diagnostics GmbH, Nonnenwald 2, DE-82377 Penzberg, Germany

2 Department of Pharmacy and Pharmacology, University of Bath, Bath BA2 7AY, UK

3 Roche Pharma Research and Early Development, Roche Innovation Center Basel, F. Hoffmann-La Roche Ltd, Therapeutic Modalities, CH-4070 Basel, Switzerland

4 Roche Pharma Research and Early Development, Pharmaceutical Sciences, Roche Innovation Center Basel, F. Hoffmann-La Roche Ltd, CH-4070 Basel, Switzerland

5 Department of Pharmacy, Pharmaceutical Technology & Biopharmaceutics, Ludwig-Maximilians University, DE-80539 Munich, Germany

the formation of immune complexes (ICs). ICs can have an effect on the pharmacokinetics (PK) of the drug, as they can be rapidly removed from circulation (6–8). Although the detailed interaction between ADA and drug to form ICs is well understood and it is well known from the literature that large ICs are cleared faster than smaller ICs, quantitative information on the exact size or structure of the formed ICs as well as their disposition has been investigated rarely so far (9–12).

Our recent publication has reported on *in vivo* studies in rats where pre-formed drug/ADA ICs were dosed to demonstrate the impact of drug/ADA ICs on drug PK by analyzing the IC pattern changes in the *in vivo* samples (7). The formed ICs consisted of dimeric, tetrameric, hexameric, octameric, and high molecular weight (HMW) ICs (Fig. 1). Rapid clearance of larger ICs (larger than hexamers) only 0.25 h after administration without dissociation into smaller ICs or their non-complexed components raised the question of where the ICs ended up in the body. To explore the effects of IC formation on the biodistribution of therapeutic mAbs, *in vivo* studies were performed. Rats were dosed with pre-formed ICs, like described in a previous publication, but using a radiolabeled drug (tritium-labeled IgG; hereafter referred to as ^{3}H-drug) and a polyclonal ADA (pADA) (7). The disposition of monomeric ^{3}H-drug was compared to ^{3}H-drug fully complexed with pADAs (hereafter referred to as "^{3}H-IC"). The radioactive label is used to gain quantitative information about the fate of the ICs by quantitative whole-body autoradiography (QWBA) and radioactive measurements of defined organs.

Materials and Methods

Reagents and Antibodies Used

The drug surrogate IgG_1 for this study was produced in-house. The polyclonal ADA surrogate $pAb_{<CDR>}$ was generated by immunization of rabbits in-house (13). Sodium chloride (1.06404) was obtained from Merck KGaA (Germany). Histidine was ordered from Sigma (H6034 and 56190). Antibodies and buffers used to generate the *in vivo* dosing solutions were tested and approved for endotoxin levels.

^{3}H-Labeling of Drug

The drug surrogate was transferred into a Slide-A-Lyzer Cassette (G2 Dialysis Cassettes, 10 K MWCO, 3 mL, Thermo Fisher Scientific, 87730) and buffer exchanged into DPBS (14 mg, 97.9 nmol, in 2.8 mL formulation buffer) (Thermo Fisher Scientific, 14190-094). The buffer was changed 4 times after 30 min and stored overnight at 6°C. The protein solution was warmed to 22°C; a protein concentration determination (Eppendorf BioSpectrometer®)

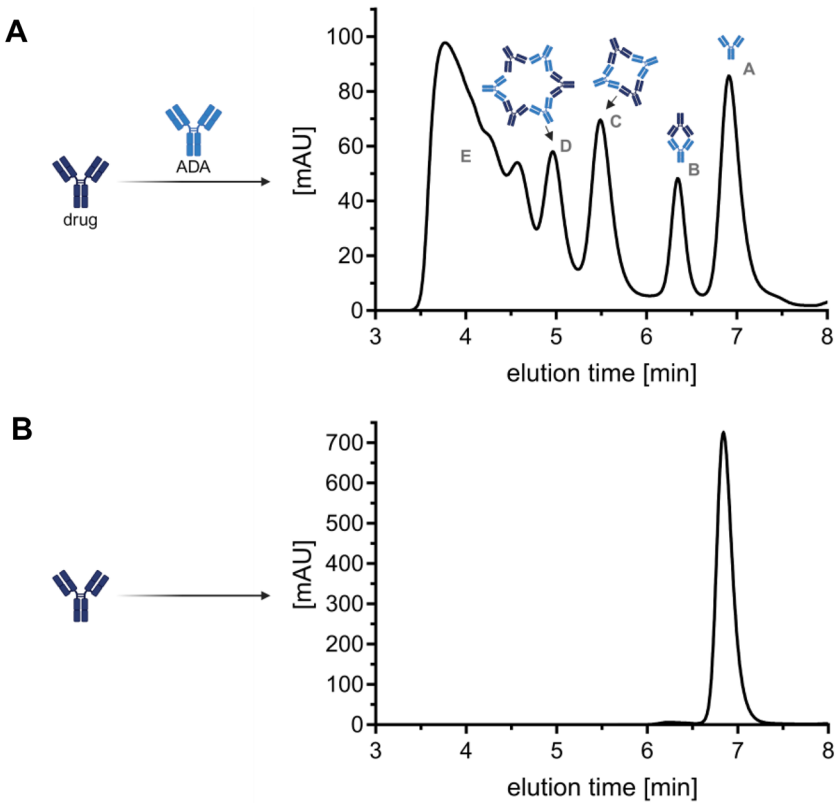

Fig. 1 Schematic illustration of different IC species and SEC of the dosing solution (^{3}H-IC), detected at 280 nm. **a** A residual, monomeric ADA, B dimeric IC, C tetrameric IC, D hexameric IC, E HMW ICs. **b** Monomeric drug

resulted in 4.9 mg/mL. Twenty-five millicuries (925 MBq, 44.5 µg, 245 nmol) [^{3}H]NSP (Pharmaron, Cardiff, Wales, UK) as a solution in toluene was transferred in portions into a 5-mL Eppendorf LoBind tube. Toluene was removed by an argon stream, and the solid residue was dissolved in 35 µL DMSO. A total of 2.8 mL of the protein solution was added, and the tube was shaken horizontally at 150 rpm for 30 min. The solution was transferred into a Slide-A-Lyzer Cassette and buffer exchanged into formulation buffer (20 mM L-histidine and L-histidine monohydrochloride monohydrate (Sigma, H-8000/H-5659), 140 mM sodium chloride (Sigma, 71376), pH 6.0). The buffer was changed 4 times after 30 min and stored overnight at 6°C. The solution was transferred to a 5-mL Eppendorf LoBind tube at 22°C and resulted in a protein concentration of 4.4 mg/mL in a volume of 2.9 mL. A total activity of 10.7 mCi (396 MBq) was obtained, resulting in a specific activity of 839 µCi/mg (31.0 MBq/mg). Radiolabeled antibody was analyzed using an Agilent 1200 series HPLC system (Santa Clara, CA, USA), equipped with β-radioactivity HPLC detector RAMONA* with internal liquid scintillator admixture (Elysia-raytest, Straubenhardt, Germany). Absorbance at 280 nm and 320 nm was used for detection and quantification. For size-exclusion chromatography (SEC), a TSKgel G3000 SW_{XL} column (Tosoh Bioscience, Tokyo, Japan), 7.8 × 300 mm, 5 µm with 0.2 M potassium phosphate, 0.25 M potassium chloride, and pH 7.0 as the mobile phase at a flow rate of 0.5 mL/min, was used. The injection volume was 10 µL and the protein concentration 1 mg/mL. The target concentration of 1 mg/mL was set by adding the eluent to the protein stock solution. The radiochemical purity using SEC was 98.1%; the low molecular weight impurity was 1%.

Analytical FcRn affinity chromatography was carried out with an FcRn affinity column (Roche Custom Biotech, Mannheim, Germany), column volume of 0.5 mL containing 1.5 mg FcRn protein (14). The 45-min analytical method was applied with a flow rate of 0.5 mL/min under the following conditions: Eluent [A] was 20 mM 2-(*N*-morpholino) ethanesulfonic acid (MES) (with 140 mM sodium chloride, pH 5.5) and eluent [B] was 20 mM tris(hydroxymethyl)aminomethane (Tris) (with 140 mM sodium chloride, pH 8.8). Starting with isocratic conditions of 20% [B] for 5 min, a linear gradient to 100% [B] followed over 35 min to keep 100% [B] for 5 min. The injection volume was 30 µL and the protein concentration 1 mg/mL. The target concentration of 1 mg/mL was set by adding eluent [A] to the protein stock solution. Liquid scintillation counting was accomplished using a HIDEX 300 SL (Mainz, Germany) and an ULTIMATE GOLD cocktail (PerkinElmer Inc., Waltham, MA, USA). A comparison of unlabeled with the tritium-labeled protein using FcRn affinity chromatography revealed no shift in retention times, which indicates that the label has no influence on FcRn affinity. The protein solution was sterile-filtered using a Millex-GV Durapore (PVDF) filter (Merck Millipore, Darmstadt, Germany), divided into two portions, and stored at − 80°C.

Generation and Characterization of Dosing Solutions

An endotoxin-free 20 mM histidine/HCl buffer (with 140 mM NaCl, pH 6) was used to generate the dosing solutions for the *in vivo* studies. For the control groups, 2 mg/mL drug was prepared. For the IC groups, a solution of 2 mg/mL drug and 3 mg/mL ADA was prepared and incubated for 1 h at 22°C on a shaker at 450 rpm before administration. Aliquots of the solutions were stored at − 80°C for further analysis by SEC using a Dionex Ultimate 3000 system like described previously (7, 10).

Study Design QWBA (Quantitative Whole-Body Autoradiography)

This study was performed at a contractor research organization. Tissue distribution and kinetics as well as blood distribution were investigated after i.v. administration of the radiolabeled drug to female rats. For this purpose, CRL:WI rats were dosed with ^{3}H-drug (4 mg/kg) or ^{3}H-drug complexed with $pADA_{<CDR>}$ (4 mg/kg and 6 mg/kg, respectively) (n = 1) and sacrificed 0.25 h after administration. The body of the animals was embedded as a whole in a frozen state. The concentration of radioactivity in tissues and organs was determined in whole-body sections of the animals by means of the QWBA technique. Just before the sacrifice, blood was taken from the sublingual vein under anesthesia (K3-EDTA). The aliquots were separated and used for the determination of total radioactivity in the blood by liquid scintillation counting (LSC) after solubilization using tissue solubilizer Solvable (PerkinElmer). Immediately, after blood sampling, the animals were sacrificed by an overdose of carbon dioxide.

QWBA: Preparation of Animal Sections

The preparation of the whole-body animal sections was performed using a cryostat microtome Cryo Macrocut Leica CM 3600 XP (Leica Instruments GmbH, Nussloch, Germany). After sacrifice, the animals were immediately frozen as a whole at approximately − 80°C in a mixture of hexane in solid carbon dioxide until the animals were completely frozen (approximately 0.5 h). Thereafter, the frozen animals were stored for at least 1 day in the deep freezer at approximately − 20°C for equilibration. The animals were then processed as soon as possible. The tail and limbs of the carcass were trimmed in a frozen state. The carcass was placed on a specimen frame. An aqueous solution of Methylan (Henkel,

Düsseldorf; 125 g/7 L tap water) was poured over the carcass. The specimen frame containing the animal was put into a freezer (− 20°C for at least 24 h). Prior to sectioning, the embedded animal was allowed to equilibrate for approximately 1–2 h to the temperature of the cryostat (− 20 ± 2°C). The frozen block was cut in a cryomicrotome at a temperature of − 20 ± 2°C. Sections of 40 µm thickness were automatically sliced to the section of interest. Prior to the removal of the section for radioluminography, a piece of adhesive transparent tape (Scotch Tape 810; 3M, Neuss, Germany) was firmly placed onto the frozen surface of the carcass in order to adhere the cut section to the tape. Sections were taken at different levels through the embedded animal. About 6–7 levels were selected to cover all tissues. The sections were dehydrated in the microtome at (− 20 ± 2°C) for at least 48 h. The sections were then treated with talcum to cover the unoccupied sections of the adhesive tape. A series of 8 blood calibration standards with different concentrations of [^{3}H]glucose plus one blank prepared with control blood was used. The concentrations of radioactivity covered a range from 10,000 to 30,000,000 dpm/g. The radioactivity of each blood calibration standard was determined after dissolving using a tissue solubilizer followed by LSC. The mean value of each standard was used to establish a calibration curve for the correlation of PSL (photo-stimulated luminescence) and dpm (radioactivity).

Biodistribution Study

All studies were conducted with the approval of the local veterinary authorities in strict adherence to the Swiss federal regulations on animal protection and to the rules of the Association for Assessment and Accreditation of Laboratory Animal Care International (AAALAC). Tissue, serum, urine, and feces distribution and kinetics were investigated after i.v. administration into the tail vein of the radiolabeled drug to female Wistar rats (CRL:WI; age approximately 8 weeks old and body weight of 230 g). For this purpose, rats were dosed with ^{3}H-drug (4 mg/kg) or ^{3}H-drug complexed with $pADA_{<CDR>}$ (4 mg/kg and 6 mg/kg, respectively) (n = 5). Blood samples were taken from the sublingual vein under anesthesia after 0.25, 1, 3, 7, 24, 48, 72, and 168 h (n = 2 per time point). For organ collection, animals were sacrificed 0.25, 3, 7, and 168 h after administration (n = 1 per time point). The liver, lung, muscle, kidney, spleen, skin, heart, bone marrow, and pancreas were collected. Urine and feces from all rats were collected in 2 blocks, from 0 to 24 h and 24 to 48 h.

Determination of Radioactivity in Serum and Organs by Liquid Scintillation Counting (LSC)

Ten microliters of serum sample were directly pipetted into a 6-mL scintillation vial (PerkinElmer, polypropylene), and 3.5 mL of Scintillation Cocktail (PerkinElmer, Ultima Gold™, 6013329) was added. The tubes were rigorously mixed using a Vortex mixer, and the radioactivity was measured using a liquid scintillation analyzer (Packard A3100). For tissue, approximately 200 mg material was transferred into Precellys24 tubes, and 3 mL of a 1:1 Soluene350/2-propanol solution was added. Samples were homogenized with the Precellys24 homogenizer three times for 10 s. An aliquot of 250 µL of the homogenates was transferred into 20-mL scintillation vials. One milliliter of a 1:1 Soluene350/2-propanol solution was added to the sample and incubated at 40°C overnight. Depending on the organ, a bleaching step was needed (e.g., kidney). In this case, 50 µL hydrogen peroxide 35% was added to the sample, and the vial was incubated at 40°C for 2 h. Fourteen milliliters of scintillation cocktail was added to the vial and rigorously mixed using a Vortex mixer, and the radioactivity was measured using a liquid scintillation analyzer (Packard A3100). Following equation is used to determine the total radioactivity per gram collected organ.

Size-Exclusion Chromatography and Reconstruction of Complex Profile by Solid Scintillation Counting

Protein separation was carried out by SEC on an Agilent 1290 Infinity II UHPLC system (Agilent Technologies Inc., Santa Clara, CA, USA) using an Acquity BEH SEC column (450 Å, 2.1 × 150 mm, Waters Corporation, Milford, MA, USA) with 100 mM sodium phosphate buffer at pH 7.4 containing 5% ethanol as mobile phase. Column oven temperature was set to 30°C. The method run time was 10 min at 250 µL/min isocratic flow. UV absorbance was measured with a diode array detector at 250 and 280 nm. Fractions were collected between 2.5 and 9.2 min every 0.07 min (17.5 µL) in a Deepwell LumaPlate-96 (PerkinElmer, Waltham, MA, USA), and radioactivity was measured by solid scintillation counting on a TopCount NXT HTS Microplate Counter (PerkinElmer, Waltham, MA, USA) after drying the plate in a rotational vacuum concentrator (Martin Christ Gefriertrocknungsanlagen GmbH, Osterode am Harz, Germany).

Peptide separation was carried out by SEC on an Agilent 1290 Infinity II UHPLC system (Agilent Technologies Inc., Santa Clara, CA, USA) using a Superdex 30 Increase (3.2 × 300 mm, Cytiva Marlborough, MA, USA) with 100 mM sodium phosphate buffer at pH 7.4 containing 5% ethanol as mobile phase. Column oven temperature was set to 25°C. The method run time was 60 min at 400 µL/min isocratic flow. UV absorbance was measured with a diode array detector at 215 and 280 nm. Fractions were collected between 37.5 and 57.5 min every 0.052 min (20.8 µL) in a Deepwell LumaPlate-384 (PerkinElmer, Waltham, MA, USA), and radioactivity was measured by solid scintillation counting on a TopCount NXT HTS Microplate Counter (PerkinElmer,

Waltham, MA, USA) after drying the plate in a rotational vacuum concentrator (Martin Christ Gefriertrocknungsanlagen GmbH, Osterode am Harz, Germany).

Results

Formation and Characterization of the Immune Complex Dosing Solution

The preparation of the dosing solutions was performed as previously described by Hoffmann and coworkers (10). As a drug surrogate, a non-targeting IgG_1 was used, which carried a mutation in the Fc part that ablated the Fc effector function (15). The drug was labeled with tritium (^{3}H-drug) in analogy to the previously reported method by conjugation of [^{3}H]*N*-succinimidyl propionate to lysine in the protein sequence (16). On average, a humanized monoclonal IgG_1 protein consists of approximately 80 lysine residues. Peptide mapping experiments identified nearly 40 lysine residues for possible conjugation (17). The study was conducted with a [^{3}H] drug with a degree of labeling (DoL) of 1.2. During the labeling process, the label was randomly distributed across the accessible lysine residues. This distribution of radiolabels on the antibody allows tracking of metabolized protein fragments.

For the dosing solution containing ICs, the ^{3}H-drug was mixed at a ratio of 1:1.5 with a polyclonal ADA surrogate directed against the CDR of the drug ($pADA_{<CDR>}$). By using a 1:1.5 ratio of drug and ADA, full complexation of drug by ADAs was ensured, which avoided free circulating drug but kept the excess of ADAs as low as possible. As the focus of the study was on drug/ADA ICs, no monomeric drug should bias the results. The use of pre-formed ICs enables us to follow directly the kinetics of the different IC sizes in serum (Fig. 3).

The dosing solution was analyzed by SEC (UV detection at 280 nm) to evaluate the pattern of formed ICs and for better comparison of the IC patterns after administration. The formed ICs consisted of dimeric, tetrameric, hexameric, and HMW ICs as depicted in Fig. 1A. Figure 1B depicts the SEC of the dosing solution for the control animals.

Quantitative Whole-Body Autoradiography (QWBA)

To quantify the distribution of radiolabeled immune complexes *in vivo*, QWBA was performed after a single-dose animal study in rats with ^{3}H-drug and ^{3}H-IC. Animals were sacrificed after 0.25 h after IV dosing. The short *in vivo* phase was based on findings from our previous work, where fast drug clearance from the circulation was observed (7). The whole-body slices were analyzed, and radioactivity in organs was quantified (Fig. 2, Table I). To provide a better comparison of the radioactive uptake of the organs, the tissue-to-blood ratio was calculated. For the control group dosed with monomeric ^{3}H-drug, the muscle, skin, stomach, and thymus revealed a low tissue-to-blood ratio of 0.01–0.06. Higher tissue-to-blood ratio was detected in the lung, liver, and kidney (medulla) accounting for 0.9, 0.34, and 0.54, respectively. In general, the total concentrations of radioactivity in the tissues were lower than in the blood.

For the animal dosed with the pre-formed ICs of ^{3}H-drug and ADA, an increased concentration of radioactivity was detected in several tissues such as the spleen (tissue-to-blood ratio of 1.21) and liver (tissue-to-blood ratio of 2.45). In other tissues such as the skin and muscle, the tissue-to-blood ratio remained low accounting for 0.04 and 0.06, respectively. For the pancreas, a high tissue-to-blood ratio of 1.37 to 3.38 was detected. The area with high radioactivity was inhomogeneous leading to a wide range.

Biodistribution Study

Like for QWBA, rats were dosed with monomeric ^{3}H-drug (control group) or with ^{3}H-drug complexed with $pADA_{<CDR>}$ (IC group) ($n = 5$ per group). Blood samples were collected after 0.25, 1, 3, 7, 24, 48, 72, and 168 h for analysis of immune complexes. Organs were collected at respective time points as described before and prepared for determination of radioactive concentration. In addition, urine and feces were collected from the animals between 0 to 24 h and 24 to 48 h to measure excreted radioactivity.

Immune Complex Analysis

To study the IC pattern changes in the collected serum samples and to compare them with the IC pattern in the dosing solution, samples from the IC group (one sample per time point) were analyzed by size-exclusion chromatography (SEC). Fractions were collected, and the radioactivity in the fractions was determined using solid scintillation counting. Figure 3 shows the reconstructed IC profiles. Direct comparison of the dosed IC pattern (Fig. 1) with the reconstructed IC pattern in serum showed that HMW and hexameric ICs disappear very fast. Dimeric and tetrameric ICs stay much longer in circulation. Between 24 and 72 h, the tetrameric IC content seemed to be very similar. The dimeric IC content showed few changes between 7 and 72 h. During the observed time, no monomeric drug was detected, indicating that ICs did not dissociate *in vivo*. This outcome is in agreement with previous data generated with the unlabeled drug (7).

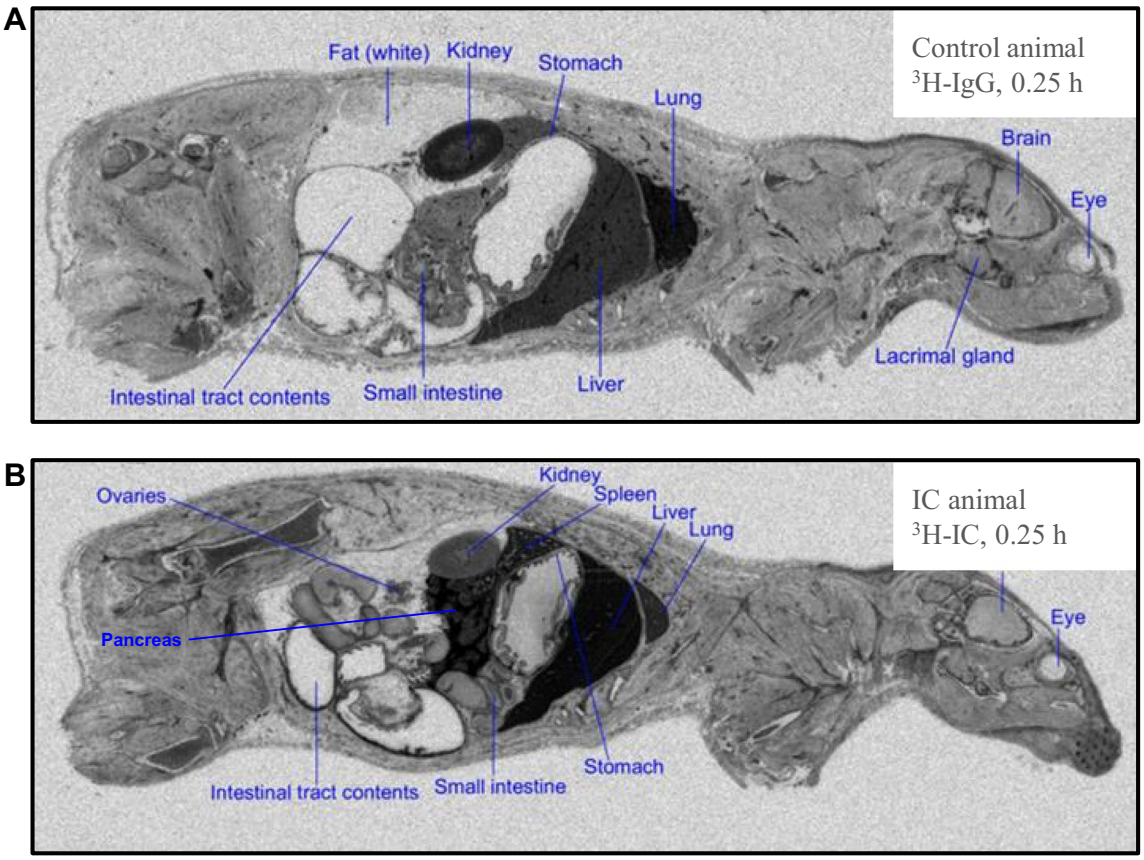

Fig. 2 Representative whole-body autoradiograms of female rats after single intravenous administration of **A** 4 mg/kg ^{3}H-drug and **B** ^{3}H-IC (4 mg/kg ^{3}H-drug and 6 mg/kg ADA)

Radioactivity in Organs

At 0.25, 3, 7, and 168 h, the liver, lung, spleen, muscle, kidney, skin, heart, bone marrow, and pancreas were collected from one animal per group. Organs were homogenized, and the radioactivity was determined by LSC. For better comparison between organs and between the groups, the ratio between organ and serum was calculated and illustrated in Fig. 4A, B. Figure 4C, D shows the absolute determined values for the control and IC groups (µ-eq/mL and µg-eq/g).

For the control group using monomeric ^{3}H-IgG$_1$, an increased radioactivity was observed in the liver after 0.25 h, followed by a rapid decrease. In all other organs studied, radioactivity slightly increased over time. At 168 h, the tissue-to-blood ratio was ranging between 0.01 and 0.07 for all tissues. The skin and muscle revealed the lowest ratios, while the lung, heart, and kidney had higher ratios (Fig. 4A, C).

For the IC group, the liver showed the highest tissue-to-serum ratio, followed by the kidney and spleen. Except for the liver, spleen, and kidney, all organs showed an increase over time of tissue to serum. The liver, spleen, and kidney had a high tissue-to-serum ratio at 3 h (Fig. 4B). The absolute values for the organs of the IC group showed a decrease of radioactivity over time with the exception of the muscle and skin, where a slight increase was detected (Fig. 4D).

Comparing the ratio of the organ to serum between the control and IC groups (Fig. 4A, B), the most significant differences were detected in the liver, muscle, spleen, and pancreas. Although the actual radioactivity in the pancreas is relatively low compared to other organs, the amount of radioactivity in the IC group is approximately 5-fold higher than in the control group (Fig. 4C, D).

Radioactivity in Urine and Feces

Figure 5 shows the percentage recovery of the administered radioactive dose in the corresponding time intervals determined by LSC. In the urine samples, the control group had a maximum of approx. 6% of the administered dose in the 0 to 24 h time interval. In contrast, approximately 65% was observed in the IC group in the first 24 h, indicating a much faster excretion of the ICs (18). For feces, the overall radioactivity was very low, with a maximum of approx. 0.3% in the IC group (0–24 h).

Table I Quantitative Evaluation of Radioactive Uptake in (ng-eq/g) (n = 1) in Organs and Tissues and Calculated Ratio of Radioactivity in Tissues to Radioactivity in Blood from the Control Animal (^{3}H-drug) and IC Animal (^{3}H-IC) After 0.25 h. Tissue-to-Blood Ratios Greater Than 0.25 Are Highlighted Blue in the Control Animal and Greater Than 1 Are Highlighted Green in the IC Animal

Tissue	Control animal		IC animal	
	(ng-eq/g)	Ratio to blood	(ng-eq/g)	Ratio to blood
Blood	55,030	1	21,357	1
Adrenal (cortex)	13,207	0.24	13,381	0.63
Adrenal (medulla)	48,626	0.88	17,790	0.83
Heart (myocardium without blood)	11,604	0.21	6608	0.31
Kidney (cortex)	26,890	0.49	6722	0.31
Kidney (medulla)	29,710	0.54	8908	0.42
Kidney (papilla)	15,505	0.28	7208	0.34
Large intestine (wall)	2897	0.05	9416	0.44
Liver	18,828	0.34	52,284	2.45
Lung	49,740	0.9	22,058	1.03
Muscle	3391	0.06	1338	0.06
Ovaries	11,533	0.21	5704	0.27
Pancreas	4423	0.08	29,318–72,227	1.37–3.38
Skin	638	0.01	795	0.04
Small intestine (wall)	6757	0.12	3820	0.18
Spleen	8303	0.15	25,854	1.21
Stomach	1204	0.02	5496	0.26
Thymus	1304	0.02	6199	0.29
Urinary bladder	2680	0.05	5595	0.26

IC immune complex

To better understand the excreted molecular substance(s) in the urine of the IC group, the urine was analyzed by peptide-level SEC determining the radioactivity in each collected fraction (Fig. 6). The radio-chromatogram of the urine showed the same pattern in the control and IC groups, but different signal intensities. The radio-chromatogram also indicated that only one species is present. A commercially available calibration standard was used to narrow down the molecular weight of the excreted substance. The radioactive substance eluted near the calibrator with a molecular weight of 1.2 kDa. Taking into consideration the impact of the spatial structure on the elution behavior, this molecular weight can only be taken as a rough approximation.

To assess whether the secreted substrate was the amino acid lysine conjugated with [^{3}H]propionate, a non-radioactive *N*-ε-propionyl lysine was used as standard and spiked into the sample. Analysis was performed by a peptide-level SEC (Fig. 6). The control *N*-ε-propionyl lysine eluted later than the substance in the urine, indicating that the unknown substance is larger than the labeled amino acid.

Discussion

The formation of immune complexes plays an important role in various preclinical and clinical aspects, like autoimmunity or immunogenicity against biotherapeutics (19).

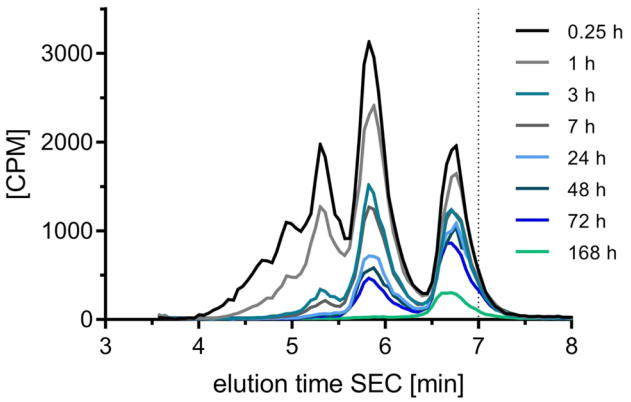

Fig. 3 ^{3}H-IC profiles of serum samples from the IC group. ^{3}H-ICs in different serum samples were separated by SEC and fractionated, and the radioactivity in the fractions was determined by LSC 0.25, 1, 3, 7, 24, 48, 72, and 168 h after administration. Potential elution of monomeric ^{3}H-drug is marked with a dashed line

Previous publications have reported investigations into the formation and characterization of drug/ADA ICs and their bioanalysis in biological matrices, as well as the impact of these ICs on the PK of antibody-based drugs (7, 10).

The question was raised as to which organ or tissue caused the fast disappearance of the immune complexes, particularly due to the fact that larger immune complexes than hexamers already cleared as early as 0.25 h post dosing (7). To investigate this question, a QWBA was performed using ^{3}H-labeled drug (non-targeting IgG_1 with a PGLALA mutation in the Fc domain ablating the Fc effector function) (control animal) or complexed with a polyclonal ADA directed against the CDR of the drug (IC animal).

We focused our studies on intravenous administration allowing us to ensure that the IC pattern we generated *in vitro* reaches circulation and monitoring changes of this pattern over time. The QWBA slide generated from the control animal after 0.25 h post dosing showed high radioactivity in the lung, kidney, and liver. On the slide of the IC animal, a very high radioactivity was observed in the lung, liver, spleen, and surprisingly also in the pancreas (Fig. 2). Although the overall tissue-to-blood ratio for the thymus, large intestine, urinary bladder, and stomach in the IC animal is relatively low compared to organs like the liver, lung, or spleen (0.26–0.44), the direct comparison to the organ-to-blood ratio for the control animal showed a meaningful difference (0.02–0.05) indicating a deposition of immune complexes (Table I). The difference in IC disposition is in

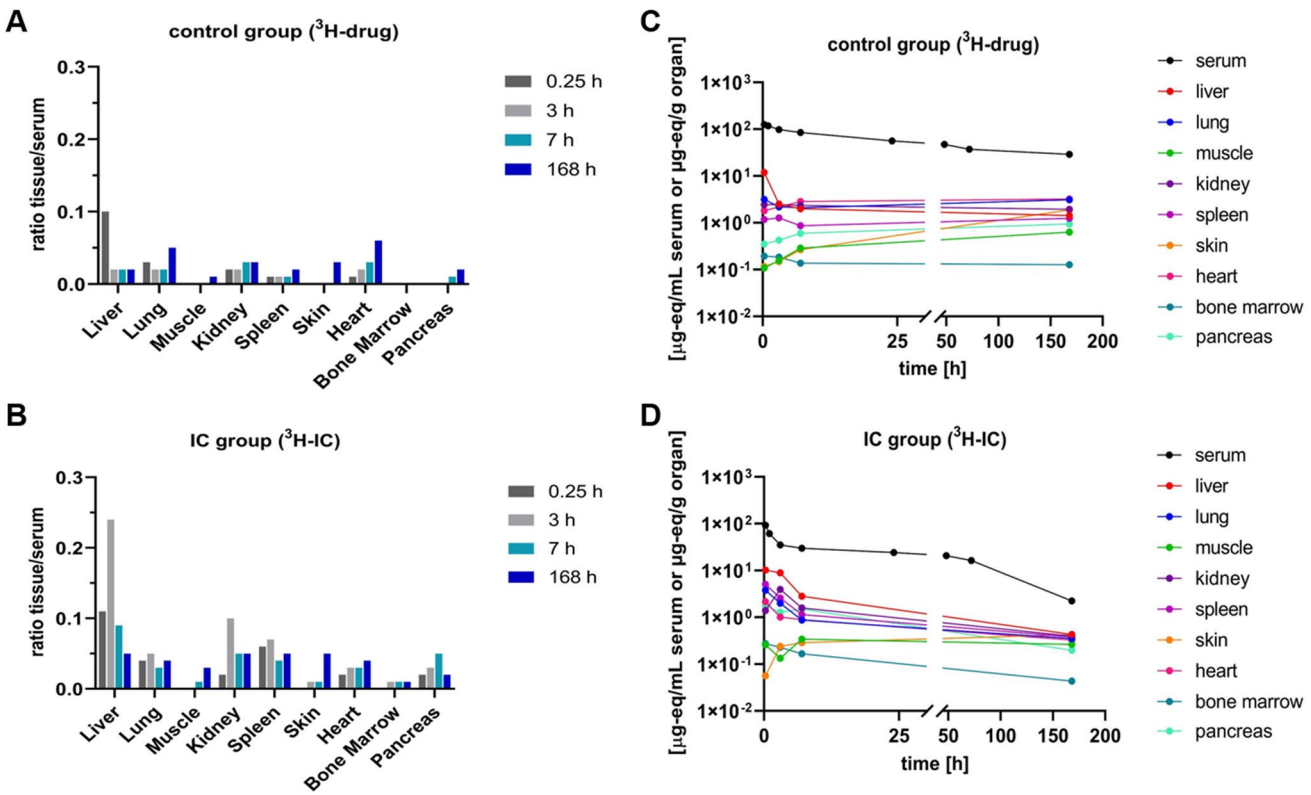

Fig. 4 Ratio between tissue/organs and serum in the control group (**A**) and the IC group (**B**). Absolute values of the detected radioactivity in collected serum and organs (log scale for *x*- and *y*-axes) in the control group (**C**) and the IC group (**D**). Serum and organs were collected at defined time points (0.25, 3, 7, and 168 h after administration), and the radioactivity was determined by LSC

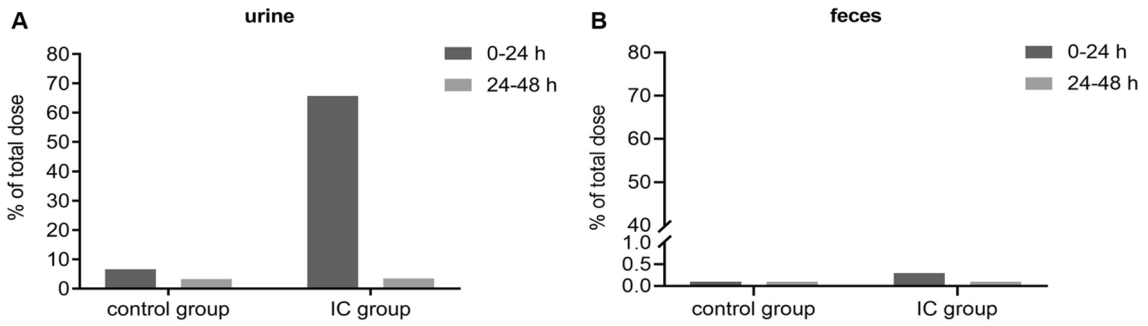

Fig. 5 Percentages of total administered dose measured in urine (**A**) and feces (**B**). Samples were collected in time frames of 0–24 h and 24–48 h. Radioactivity was determined by LSC

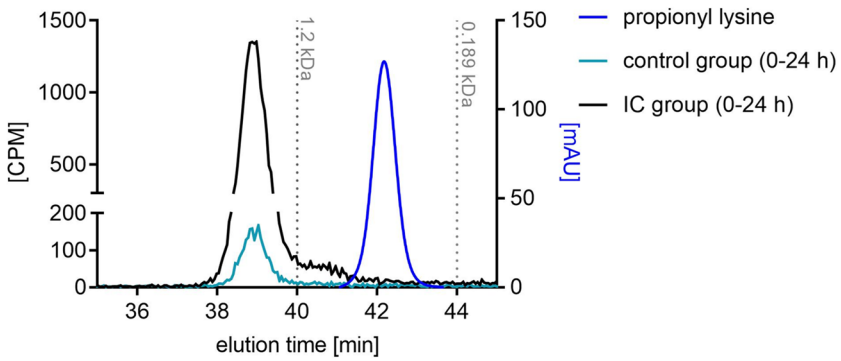

Fig. 6 Peptide SEC analysis of collected urine (0–24 h) of the control and IC groups with radioactive readout (CPM). In addition, non-radioactive *N*-ε-propionyl lysine was injected as control (mAU) at 215 nm. The dashed lines mark the elution of the SEC standards in the area of interest (vitamin B12: 1.2 kDa; triglycine: 0.189 kDa)

line with current knowledge about the location of the reticuloendothelial system (RES) mainly in the liver, lung, and spleen.

Involvement of the pancreas was not expected, as there was no evidence found in the literature to suggest that the pancreas could play a role in IC disposition or metabolism. To confirm the findings from the QWBA, a follow-up study was performed using a different readout. The same ^{3}H-drug, pADA, and dosing regimen were used but with more sampling time points. After 0.25, 3, 7, and 168 h, one animal per group was sacrificed, and serum and defined organs were taken for further analysis. Serum samples from the IC group were separated by SEC and fractionated, and the radioactivity in the fractions was subsequently measured to reconstruct the immune complex pattern (7, 10). The reconstructed immune complex patterns indicated that already after 0.25 h, most HMW ICs were cleared from circulation (Fig. 3). The dimeric immune complex, on the other hand, was detectable even after 168 h. The results confirm well to the previous study, which used the same molecules without radioactive labeling (7). The immune complex patterns in the former study were determined using SEC followed by a drug-specific ELISA. The comparison of the previous study and the study presented here also demonstrated that the readout (LSC/radioactivity *vs.* drug-specific ELISA) had no impact on the reconstructed immune complex pattern (data not shown). The collected organs were homogenized, and the radioactivity was determined by LSC. For better comparison, the radioactivity in the organs was normalized by the radioactivity in serum.

Similar to the QWBA study, the control animals showed increased radioactivity in the liver, lung, and kidney after 0.25 h. Over time, radioactivity increased in the lung, kidney, heart, and pancreas (Fig. 4A). For the IC group, the liver, lung, and spleen showed the highest radioactivity after 0.25 h, as in the QWBA (Fig. 4B) (18, 20). Overall, the ratio of serum to tissue was much lower than previously obtained by QWBA. The values obtained by QWBA are in line with previously published data (21). These differences can be explained by the residual blood levels, which remain in the organ after euthanasia of the animal. As depicted in Fig. 4, the serum levels are 10–100 times higher than in tissue as a result of the low extravasation of antibodies. For both applied techniques, QWBA and biodistribution without perfusion, the confounding factor of residual blood is known. The main objective was to identify organs that show higher uptake of immune complexes rather than to determine absolute ("true") levels of tissue concentrations.

Interestingly, although in the biodistribution study, radioactivity in the pancreas was up to five times higher than in the control group, it appeared to be less pronounced compared to the very high radioactivity observed in the

QWBA study. The increase of radioactivity over time (up to 7 h) indicates an accumulation in the pancreas. These results could be explained in two ways; the pancreas is taking up immune complexes, or the immune complexes were proteolyzed in the liver, and then, the radiolabeled amino acid or peptides were taken up by the pancreas because of its high protein expression level (22). In the case of the second option, this would presume that the ^{3}H-labeled amino acid could be reused during the protein expression and processed into new proteins by the natural protein expression machinery. This would also explain why the radioactivity in the control animal also increased over time. The monomeric IgG is taken up as part of endogenous processes and degraded by proteolysis. This process is much slower compared to immune complexes. Assuming reuse of the labeled amino acid for new proteins, the high amount of radioactivity in the pancreas was not caused in the first instance by the disposition of the immune complexes, but as secondary an effect of the increased proteolytic digestion of the immune complexes in the liver and subsequent uptake for protein synthesis.

In the biodistribution study, the collected urine of the IC animals indicated that 65% of the dosed radioactivity was excreted within the first 24 h, compared to only 6% for the control group (Fig. 5) (18). This is a clear hint that immune complexes are internalized, proteolytically digested, and excreted much faster than monomeric IgG.

Interestingly, although the drug was randomly labeled via conjugation to lysine residues, only one distinct peak was identified in a peptide SEC analysis with a radioactive readout, indicating the presence of one molecular species (Fig. 6). This radioactive species was found in both the IC and control groups. To better estimate the size of this species, a commercial SEC standard was used, but also *N*-ε-propionyl lysine, which mimics a proteolyzed lysine residue after ^{3}H-propionylation on the endogenous nitrogen (Fig. 6). The results suggest that the radioactive species in urine is not the monomeric labeled lysine, but rather a molecular size of approximately 1.2 kDa (excluding the impact of the spatial structure on the elution behavior), indicating that the species is a peptide consisting of several amino acids. The fact that only one species was found, although a random labeling of drug lysine residues was performed, could be due to insufficient separation of the potentially different species present by the peptide SEC used. Further analysis of the urine will be needed to study more deeply the actual species present.

Comparison of the 0.25 h results from the QWBA and the biodistribution study confirmed that the liver, as expected, is the central organ for immune complex clearance in the first minutes, followed by the spleen (Fig. 4, Table I). It can be concluded that the follow-up biodistribution study with improved sampling time points and study duration contributed significantly to obtaining a better picture of the processes during biodistribution and completing the results of the QWBA study.

Rojas *et al*. (12) also reported 2005 accelerated clearance of drug/ADA ICs. However, this study did not address additional aspects we focused on. The used drug (infliximab) is a human/murine chimeric and does not represent the properties of modern humanized therapeutic antibodies with engineered Fc effector functions. Furthermore, the study by Rojas *et al*. had a different objective by investigating the *in vivo* formation of ICs and their distribution and elimination resulting from a low-level immune response in the presence of excess drug. They also used a different approach of IC formation (*in vivo vs.* our *in vitro* approach), a different animal test model, and a lower total radioactive dose. Furthermore, the labeling chemistry (direct iodination *vs.* NHS) applied was different. As described by Edelmann and Hauri (2021) (14), direct iodination could harm an antibody due to the harsh oxidative reaction condition, which can lead to a higher clearance. In comparison, tritium-labeled propionate has less impact on biological behavior. All these aspects make a direct comparison and simple transfer of the results very challenging to impossible. Nevertheless, the findings are in agreement with our findings

Conclusions

To investigate the *in vivo* behavior of immune complexes (ICs) of drug/ADAs, a drug-like IgG was labeled with tritium and treated with an anti-IgG antibody directed against the CDR. A biodistribution study and a QWBA study were performed with the ^{3}H-drug and the ^{3}H-IC in rats. These studies confirmed that drug/ADA immune complexes are removed from the circulation faster than the drug-like IgG. Up to now, it was not clear where and when these ICs are distributed or excreted in the body. A finding of these biodistribution studies with tritium-labeled compounds was that an increased level of radioactivity accumulates in the pancreas. To the best of our knowledge, this accumulation has been observed in the pancreas for the first time. Furthermore, a high amount of radioactivity from the group receiving the pre-complexed ^{3}H-IC dose was found in the urine in the first 24 h. So far, it has not been possible to identify the main degradation product. Estimation was possible only with a molecular weight marker using SEC, which showed a peptide of a size of approximately 1.2 kDa. Further investigations are required in order to gain a greater understanding of the degradation of IC.

Acknowledgements The authors want to thank Christelle Rapp, Marie Stella Gruyer, Veronique Dall' Asen, Thorsten Muser, and Thomas Ramp (Roche Pharmaceutical Research and Early Development, Roche Innovation Center Basel, Switzerland) for their support in conducting animal experiments, radiolabeling, and radio-chromatographic

analysis. The authors thank Dr. Filippo Sladojevich from F. Hoffmann-La Roche AG, Basel, as well as Prof. Stephen M. Husbands and Dr. Ian S. Blagbrough from the University of Bath for providing valuable comments and reviews on the manuscript.

Author Contribution Eugenia Opolka-Hoffmann, Gregor Jordan, Michael Otteneder, Martin Lechmann, and Roland F. Staack substantially contributed to the conception and design of the work. Martin Edelmann performed radioactive labeling of the drug surrogate. Peter Schrag, Simon Hauri, and Eugenia Opolka-Hoffmann substantially contributed to the experimental analysis. Eugenia Opolka-Hoffmann, Gregor Jordan, Roland F. Staack, and Michael Otteneder substantially contributed to data analysis and data interpretation. Martin Edelmann and Eugenia Opolka-Hoffmann drafted the first versions of the manuscript. All authors subsequently contributed to drafting or revising the content. All authors approved the submitted version. All authors agree to be accountable for all aspects of the work in ensuring that questions related to the accuracy or integrity of any part of the work are appropriately investigated and resolved.

Funding This project was funded by the Roche Diagnostics GmbH. E. Opolka-Hoffmann received a grant from Roche Diagnostics GmbH during her employment at the LMU.

Data Availability The datasets used and/or analysed during the current study are available from the corresponding author on reasonable request.

Declarations

Conflict of Interest E. Opolka-Hoffmann, G. Jordan. M. Lechmann, and R. F. Staack are employees of Roche Diagnostics GmbH, Penzberg. M. R. Edelmann, M. B. Otteneder, S. Hauri, and P. Schrag are employees of Hoffmann-La Roche AG, Basel. Some authors are owners of Roche bonus shares.

Ethics approval The QWBA study was authorized by the District Government of Upper Bavaria in accordance with § 8 Abs.1 of the German Animal Welfare Act. The biodistribution study was performed with the permission of the Swiss Cantonal Veterinary Office of Basel City.

References

1. Grilo AL, Mantalaris A. The increasingly human and profitable monoclonal antibody market. Trends Biotechnol. 2019;37(1):9–16.
2. Krishna M, Nadler SG. Immunogenicity to biotherapeutics–the role of anti-drug immune complexes. Front Immunol. 2016;7:21.
3. Stubenrauch K, Künzel C, Vogel R, Tuerck D, Schick E, Heinrich J. Epitope characterization of the ADA response directed against a targeted immunocytokine. J Pharm Biomed Anal. 2015;114:296–304.
4. Harding FA, Stickler MM, Razo J, DuBridge R. The immunogenicity of humanized and fully human antibodies: residual immunogenicity resides in the CDR regions. MAbs. 2010;2(3):256–65.
5. Cassinotti A, Ardizzone S, Porro GB. Adalimumab for the treatment of Crohn's disease. Biologics. 2008;2(4):763.
6. Ponce R, Abad L, Amaravadi L, Gelzleichter T, Gore E, Green J, et al. Immunogenicity of biologically-derived therapeutics: assessment and interpretation of nonclinical safety studies. Regul Toxicol Pharmacol. 2009;54(2):164–82.
7. Opolka-Hoffmann E, Jordan G, Otteneder M, Kieferle R, Lechmann M, Winter G, et al. The impact of immunogenicity on therapeutic antibody pharmacokinetics: a preclinical evaluation of the effect of immune complex formation and antibody effector function on clearance. MAbs. 2021;13(1):1995929.
8. Chirmule N, Jawa V, Meibohm B. Immunogenicity to therapeutic proteins: impact on PK/PD and efficacy. AAPS J. 2012;14(2):296–302.
9. van Schie KA, Kruithof S, Ooijevaar-de Heer P, Derksen NI, van de Bovenkamp FS, Saris A, et al. Restricted immune activation and internalisation of anti-idiotype complexes between drug and antidrug antibodies. Ann Rheum Dis. 2018;77(10):1471–9.
10. Hoffmann E, Jordan G, Lauer M, Ringler P, Kusznir EA, Rufer AC, et al. Generation, characterization, and quantitative bioanalysis of drug/anti-drug antibody immune complexes to facilitate dedicated in vivo studies. Pharm Res. 2019;36(9):1–15.
11. Rojko JL, Evans MG, Price SA, Han B, Waine G, DeWitte M, et al. Formation, clearance, deposition, pathogenicity, and identification of biopharmaceutical-related immune complexes: review and case studies. Toxicol Pathol. 2014;42(4):725–64.
12. Rojas JR, Taylor RP, Cunningham MR, Rutkoski TJ, Vennarini J, Jang H, et al. Formation, distribution, and elimination of infliximab and anti-infliximab immune complexes in cynomolgus monkeys. J Pharmacol Exp Ther. 2005;313(2):578–85.
13. Staack RF, Stracke JO, Stubenrauch K, Vogel R, Schleypen J, Papadimitriou A. Quality requirements for critical assay reagents used in bioanalysis of therapeutic proteins: what bioanalysts should know about their reagents. Bioanalysis. 2011;3(5):523–34.
14. Edelmann MR, Hauri S. Functional in vitro assessment of modified antibodies: impact of label on protein properties. PLoS One. 2021;16(9):e0257342.
15. Schlothauer T, Herter S, Koller CF, Grau-Richards S, Steinhart V, Spick C, et al. Novel human IgG1 and IgG4 Fc-engineered antibodies with completely abolished immune effector functions. Protein Eng Des Sel. 2016;29(10):457–66.
16. Edelmann MR, Kettenberger H, Knaupp A, Schlothauer T, Otteneder MB. Radiolabeled IgG antibodies: impact of various labels on neonatal Fc receptor binding. J Label Compds Radiopharm. 2019;62(11):751–7.
17. Wang L, Amphlett G, Blättler WA, Lambert JM, Zhang W. Structural characterization of the maytansinoid–monoclonal antibody immunoconjugate, huN901–DM1, by mass spectrometry. Protein Sci. 2005;14(9):2436–46.
18. Johansson A, Erlandsson A, Eriksson D, Ullén A, Holm P, Sundström BE, et al. Idiotypic–anti-idiotypic complexes and their in vivo metabolism. Cancer. 2002;94(S4):1306–13.
19. Edelmann MR. Radiolabelling small and biomolecules for tracking and monitoring. RSC Adv. 2022;12(50):32383–400.
20. Pastuskovas CV, Mallet W, Clark S, Kenrick M, Majidy M, Schweiger M, et al. Effect of immune complex formation on the distribution of a novel antibody to the ovarian tumor antigen CA125. Drug Metab Dispos. 2010;38(12):2309–19.

21. Wang M, Zhan Y, O'Neil SP, Harris S, Henson C, McEwen A, et al. Quantitative biodistribution of biotherapeutics at whole body, organ and cellular levels by autoradiography. Bioanaly. 2018;10(18):1487–500.
22. Sepp A, Meno-Tetang G, Weber A, Sanderson A, Schon O, Berges A. Computer-assembled cross-species/cross-modalities two-pore physiologically based pharmacokinetic model for biologics in mice and rats. J Pharmacokinet Pharmacodyn. 2019;46(4):339–59.